Z. Phys. C – Particles and Fields 48, 301–308 (1990)

Zeitschrift für Physik C Particles and Fields

Weak boson plus jet production in 2nd-order QCD

F.T. Brandt, G. Kramer, Su-Long Nyeo

II. Institut für Theoretische Physik, Universität Hamburg, Luruper Chaussee 149, D-2000 Hamburg 50, Federal Republic of Germany

Received 24 April 1990

Abstract. We calculate cross sections for the production of $W^{\pm}$ and Z bosons in association with 1 and 2 jets at $p\bar{p}$ collider energies. The expected rates for these processes in second-order QCD are presented as a function of the cuts on the transverse momenta of the jets and are compared with jet rates measured by UA1.

1 Introduction

Recently there has been much interest in multi-jet production in high energy processes. In particular studies of jet production in electron-positron annihilation have given us much information about the properties of quarks and gluons and the nature of their interactions as described by QCD. Now that the hadronic production of $W^{\pm}$'s, Z's is being frequently observed at the $p\bar{p}$ colliders at CERN and FNAL it is of interest to study the hadronic production of $W^{\pm}$, Z or γ^*, where γ^* is a photon with large off-shell mass, accompanied by a finite number of jets: $p+\bar{p}\to W^{\pm}$, Z, γ^*+n jets. Measurements of jet rates f_n for W production for $n=0,1,2,3$ and 4 and for Z production for $n=0,1$ and 2 have been presented by the UA1 collaboration [1]. Data on W production and jets for $n=0$ and 1 have also been published by the UA2 collaboration [2].

On the theoretical side, several authors have calculated the jet cross sections for $p+\bar{p}\to W,Z+1,2,3$ jets at the tree level [3,4] and found reasonably good agreement with data from the CERN $p\bar{p}$ collider. Now it is well known that higher order corrections are large for the Drell–Yan process. Already the first order correction $O(\alpha_s)$ changes the lowest order Drell–Yan cross section by a factor 1.5–2.0 depending on the total c.m. energy. At $O(\alpha_s^2)$ the correction to the total Drell–Yan cross section is somewhat smaller but still appreciable as was found recently [5]. Therefore we must expect similar corrections for jet cross sections in the Drell–Yan process. The purpose of this paper is to calculate the $O(\alpha_s^2)$ corrections to the cross section $p+\bar{p}\to W,Z+1$ jet for $Sp\bar{p}S$ and Tevatron energies. For this we need the complete $O(\alpha_s^2)$ matrix elements including virtual and real corrections. They describe the sum of one- and two-jet production. These second-order corrections have been calculated some time ago for the special case of the non-singlet contribution to $q\bar{q}$ annihilation by Ellis et al. [6]. These are the most important contributions at CERN energies. At Tevatron energies, however, quark-gluon scattering is equally important. This process has been investigated for the specific case $qg\to W+2$ jet at tree level [3,4]. The complete $O(\alpha_s^2)$ matrix elements for all subprocesses $q\bar{q}$, qq, qg, $\bar{q}g$, $gg\to(W,Z+1$ jet) and $(W,Z+2$ jet) are available now. They have been calculated by two independent groups, Arnold and Reno [7] and Gonsalves et al. [8], and agree with each other. We use for our evaluation of the jet cross sections the results as presented in [8]. In these calculations the polarizations of the W and Z bosons are summed.

The remainder of this paper is organized as follows. In Sect. 2 we fix our notation and describe the input of our calculation, in particular the structure functions, which we used and the definition of the cuts to define the 1- and 2-jet cross sections. In this section we also present our results and compare with results of other authors where available. We calculate the cross sections at $\sqrt{S}=0.63$ and 1.8 TeV for $W^{\pm}$ and Z production. In Sect. 3 we summarize our results.

2 Input and definition of jets

A. Parton model and kinematics

In this section we define the general structure of the cross sections for the production of an electroweak boson V, i.e. $W^{\pm}$, Z or a virtual photon, within the framework of perturbative QCD. We mostly follow [8] also in our notation. The four-momenta of the colliding hadrons are P_1 and P_2 while those of the colliding partons are $p_1=x_1P_1$ and $p_2=x_2P_2$: Q is the four-momentum of the produced vector boson V, Q_T its transverse momentum. In the QCD improved parton model the inclusive

cross section for the process

$$h_1(P_1) + h_2(P_2) \to V(Q) + X \tag{1}$$

is obtained from

$$\frac{d^3\sigma}{d^3Q} = \sum_{a_1,a_2} \int_0^1 dx_1 \int_0^1 dx_2 f_{a_1}^{h_1}(x_1, M^2) f_{a_1}^{h_2}(x_2, M^2) \cdot \frac{d^3\sigma^{a_1 a_2}}{d^3Q}(p_1, p_2, M^2). \tag{2}$$

In (2) a and b stand for quarks, antiquarks and gluons, $f_a^h(x, M^2)$ is the probability density for finding parton a with momentum fraction x in hadron h if it is probed at scale M^2, and $\sigma^{a_1 a_2}(p_1, p_2, M^2)$ is the perturbative cross section for the process

$$a(p_1) + b(p_2) \to V(Q) + X \tag{3}$$

given as a series in the strong coupling constant α_s and from which collinear singularities from radiation off massless partons have been factorized out at scale M^2 and implicitly included in the scale-dependent parton densities $f_a^h(x, M^2)$ in the usual way [9]. The Mandelstam variables for the hadron and parton processes are

$$S = (P_1 + P_2)^2, T = (P_1 - Q)^2, U = (P_2 - Q)^2$$

$$s = (p_1 + p_2)^2, t = (p_1 - Q)^2, u = (p_2 - Q)^2$$

$$S_2 \equiv S + T + U - Q^2, s_2 \equiv s + t + u - Q^2.$$

Here S_2 and s_2 are the invariant masses of the system recoiling against V at the hadron and parton levels, respectively. The hard-scattering cross section σ^{ab} is expressed in term of the variables s, t, u and s_2 which can be expressed in terms of S, T, U and Q^2 using $p_i = x_i P_i$. The relevant formulae can be found for example in [6].

B. Jet cross sections

In zeroth order of α_s the hard-scattering cross section $\sigma^{a_1 a_2}$ describes the transition $q\bar{q} \to V$ which leads just to the projectile plus target jet, which we shall not count in the following. Thus in the lowest order we have only V production with no additional extra jet. This cross section is denoted σ_0. Sometimes it will be used to normalize the higher-order cross sections. In first order of α_s an additional parton, quark, antiquark or gluon can be produced which we count as one jet if this extra parton fulfils appropriate resolution criteria. In this order of α_s there appear also virtual corrections to the $q\bar{q}V$ vertex which produce $O(\alpha_s)$ corrections to the zero-jet cross section. This contribution has infrared and collinear singularities which are cancelled against the infrared and collinear singularities of the single gluon production graphs. The remaining collinear singularities must be absorbed into the structure functions [10]. To achieve the cancellation between virtual and real contribution forces us to introduce cuts already on the partonic level. These cuts on the perturbative final state are the basis of the partonic jet definition. In the following a jet is defined in terms of a parton with a minimum $p^j{}_T$ separated from other partons by a relative angle. Of course in $O(\alpha_s)$ the minimum $p^j{}_T$ is sufficient to separate the one-jet from the zero-jet contribution. The two-jet cross section comes from the tree diagrams of order $\alpha_s{}^2$. Here $p^j{}_T > p^j{}_{T\min}$ for both outgoing partons and angular separation ω_{12} between the two partons larger than some minimal value $\omega_{\min}$ defines the two-jet contribution. The complement gives the contributions to the one-jet and zero-jet cross sections.

The angular cut controls the collinearity associated with bremsstrahlung configurations coming from outgoing quarks or antiquarks, while the requirement of a minimum $p^j{}_T$ of the jets prevents the emission of partons which are arbitrary soft or collinear with the incoming partons. With these cuts, the initial and final state partons in the $O(\alpha_s{}^2)$ tree diagrams are separated and the resulting perturbative 2-jet cross sections are finite. In the complement singularities are cancelled by the corresponding $O(\alpha_s{}^2)$ virtual corrections.

The full calculation of the $O(\alpha_s{}^2)$ corrections requires the knowledge of two-loop virtual corrections. Although they are known [5, 11] the separation of the zero-jet from the one-jet cross section in $O(\alpha_s{}^2)$ is a very lengthy calculation and has not been done yet. Actually this is not required. The existing $O(\alpha_s{}^2)$ results [6–8] provide us with the inclusive cross section, i.e. the sum of the 1-jet and 2-jet cross sections. By subtracting the 2-jet cross section which we obtain by applying the resolution cuts described above on the tree-level diagrams we obtain the $O(\alpha_s{}^2)$ correction to the one-jet cross section. Instead of the angle cut we shall use a cut on $\Delta R = (\Delta\varphi^2 + \Delta\eta^2)^{1/2}$, where φ is the azimuthal angle and η the pseudorapidity.

In the experiment the jet accompanying the vector boson V consists of hadrons which are supposed to originate from the fragmentation of the primordial partons. Thus experimentally the number of jets is equal to the number of hadron jets. But the number of reconstructed hadron jets is not necessarily equal to the number of produced partons. Depending on the specific jet definition the number of hadronic jets in an event will be larger than the number of partonic jets underlying this event. This mismatch can be resolved by running extensive Monte Carlo programs based on the perturbative cross sections and fragmentation routines which are adjusted to reproduce correctly the experimental energy flow distributions. This has been done, for example, for the jets observed in the UA2 experiment [2]. We shall not consider this problem, since fragmentation is not the only effect which must be considered if one wants to deduce the number of partonic jets from the number of experimentally observed hadron jets. On the other hand the resolution cuts on the partonic jets introduced above seem to mimic the actual cuts applied to the full hadronic final states closely enough so that the number of partonic jets is very near to the number of hadronic jets. Otherwise detailed fragmentation corrections must be calculated in connection with the specific experimental conditions and this goes beyond the purpose of this paper.

C. Parton densities

The most important phenomenological input needed for making numerical predictions is the parton density

$f_a^h(x, M^2)$. We shall employ the parton distributions of Martin, Roberts and Stirling (MRS) [12]. These distributions have been derived from deeply inelastic scattering data on the basis of the full next-to-leading-order analysis with $\overline{\text{MS}}$ prescription. We use the MRS EB mode 2 with $\Lambda_{\overline{\text{MS}}} = 0.2\,\text{GeV}$, corresponding to the fit to the BCDMS data. As scale M^2 we use $M^2 = Q^2 = {M_W}^2, {M_Z}^2$. The factorization scheme is also $\overline{\text{MS}}$ appropriate to the MRS parton densities.

3 Results

Before we subtract the 2-jet cross section from the inclusive (1 + 2)-jet cross section we give an overview of the 2-jet cross section with various cuts ${p^j}_{T\min}$ of the jets and compare them with the inclusive cross section. We do this for W and Z production and for the two c.m. energies of interest, $\sqrt{S} = 0.63\,\text{TeV}$ and $\sqrt{S} = 1.8\,\text{TeV}$. For W production we add the cross section for W^+ and W^-, since only this has been measured so far. The coupling α_s is calculated with $\Lambda_{\overline{\text{MS}}} = 0.2\,\text{GeV}$ from the functional form given in [13]. The scale is equal to ${M_W}^2$ and ${M_Z}^2$ respectively. We use $M_W = 80.27\,\text{GeV}$ and $M_Z = 91.17\,\text{GeV}$. The cuts on the 2-jet contribution are $\Delta R \geqq 1.0$ ($\sqrt{S} = 0.63\,\text{TeV}$) and $\Delta R \geqq 0.7$ ($\sqrt{S} = 1.8\,\text{TeV}$) with $|\eta| \leqq 2.5$ and with varying ${p^j}_{T\min}$ of the transverse momentum ${p^j}_T$ of the jets. Results for these cross sections are shown in Fig. 1a, 2a, 3a and 4a. In Fig. 1a and 2a the curves are for $\sqrt{S} = 0.63\,\text{TeV}$ and for W and Z production respectively. The ${p^j}_{T\min} = 2.5$, 5.0, 10.0 and 15.0 GeV. All cross sections are given as a function of the V transverse momentum p_T and are normalized by σ_0. The dotted, continuous curve is the inclusive cross section. We see that for cuts ${p^j}_{T\min} \geqq 5\,\text{GeV}$ the two-jet cross section is always very much smaller than the inclusive cross section so that for these larger cuts the inclusive cross section is almost exclusively one-jet. The inclusive cross section contains

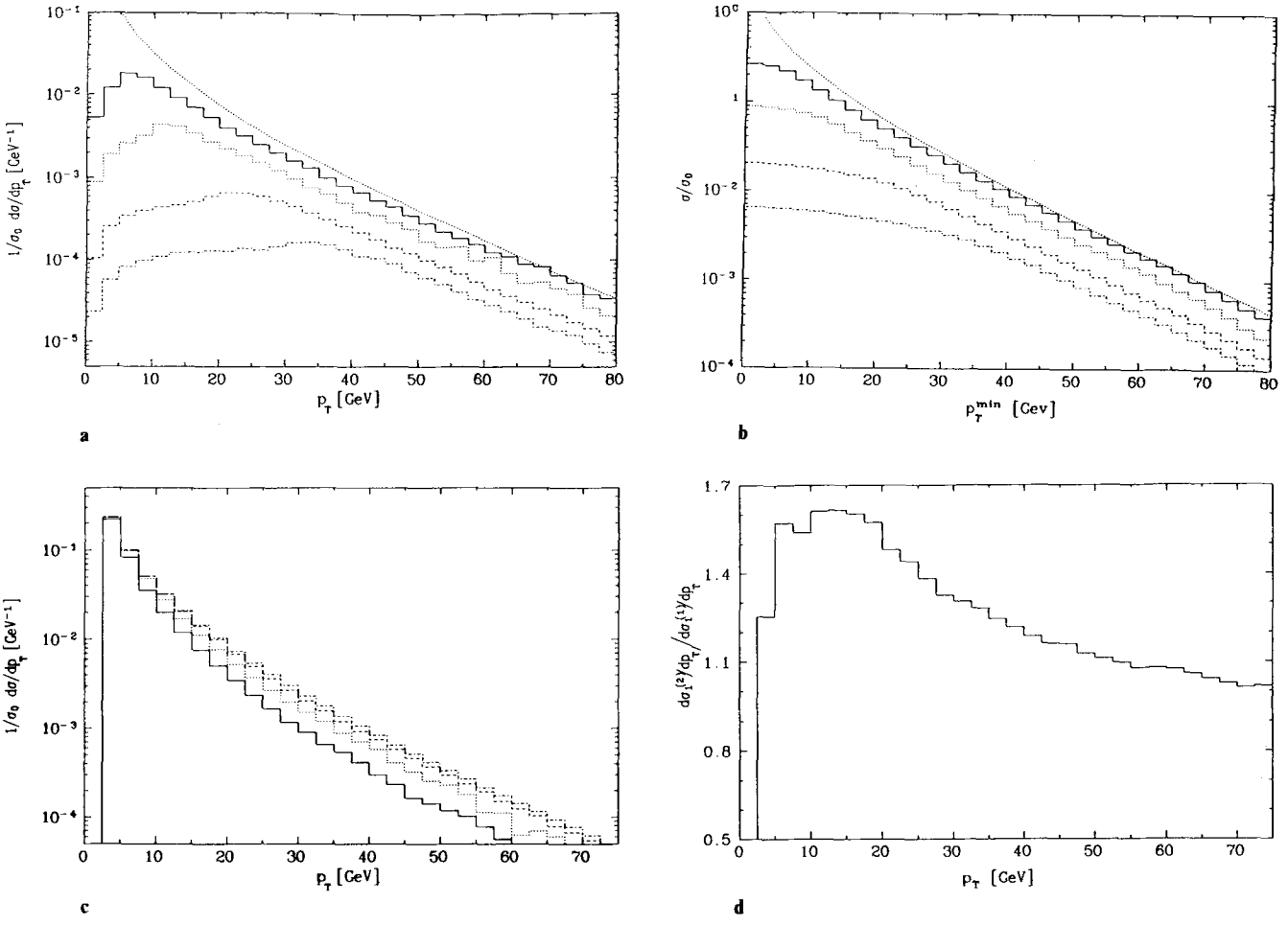

Fig. 1. **a** The inclusive transverse momentum distribution (dotted curve) ((1 + 2)-jet) as a function of the vector boson p_T for W production at $\sqrt{S} = 0.63\,\text{TeV}$ compared to the 2-jet p_T distributions for ${p^j}_T \geqq 2.5\,\text{GeV}$ (full histogram), 5 GeV (dotted histogram), 10 GeV (dashed histogram), 15 GeV (dashed-dotted histogram) and for $\Delta R \geqq 1.0$, $|\eta| \leqq 2.5$. All cross sections are divided by σ_0 ($\sigma_0 = 4.643\,\text{nb}$). **b** The integrated (1 + 2)- and 2-jet rates as a function of the lower limit ${p_T}^{\min}$ for various cuts on ${p^j}_T$, normalized by σ_0. Labelling of histograms as in Fig. 1a for W production at $\sqrt{S} = 0.63\,\text{TeV}$. **c** The $O(\alpha_s)$ and $O({\alpha_s}^2)$ 1-jet transverse momentum distributions as a function of the p_T of the W boson at $\sqrt{S} = 0.63\,\text{TeV}$ for ${p^j}_T \geqq 2.5$, 5, 10, 15 GeV, $\Delta R \geqq 1$, $|\eta| \leqq 2.5$. Labelling of histograms as in **a**. **d** Ratio of $O(\alpha_s) + O({\alpha_s}^2)$ to $O(\alpha_s)$ p_T distribution for W + 1-jet for $\sqrt{S} = 0.63\,\text{TeV}$, ${p^j}_T > 10\,\text{GeV}$, $\Delta R \geqq 1.0$ and $|\eta| \leqq 2.5$

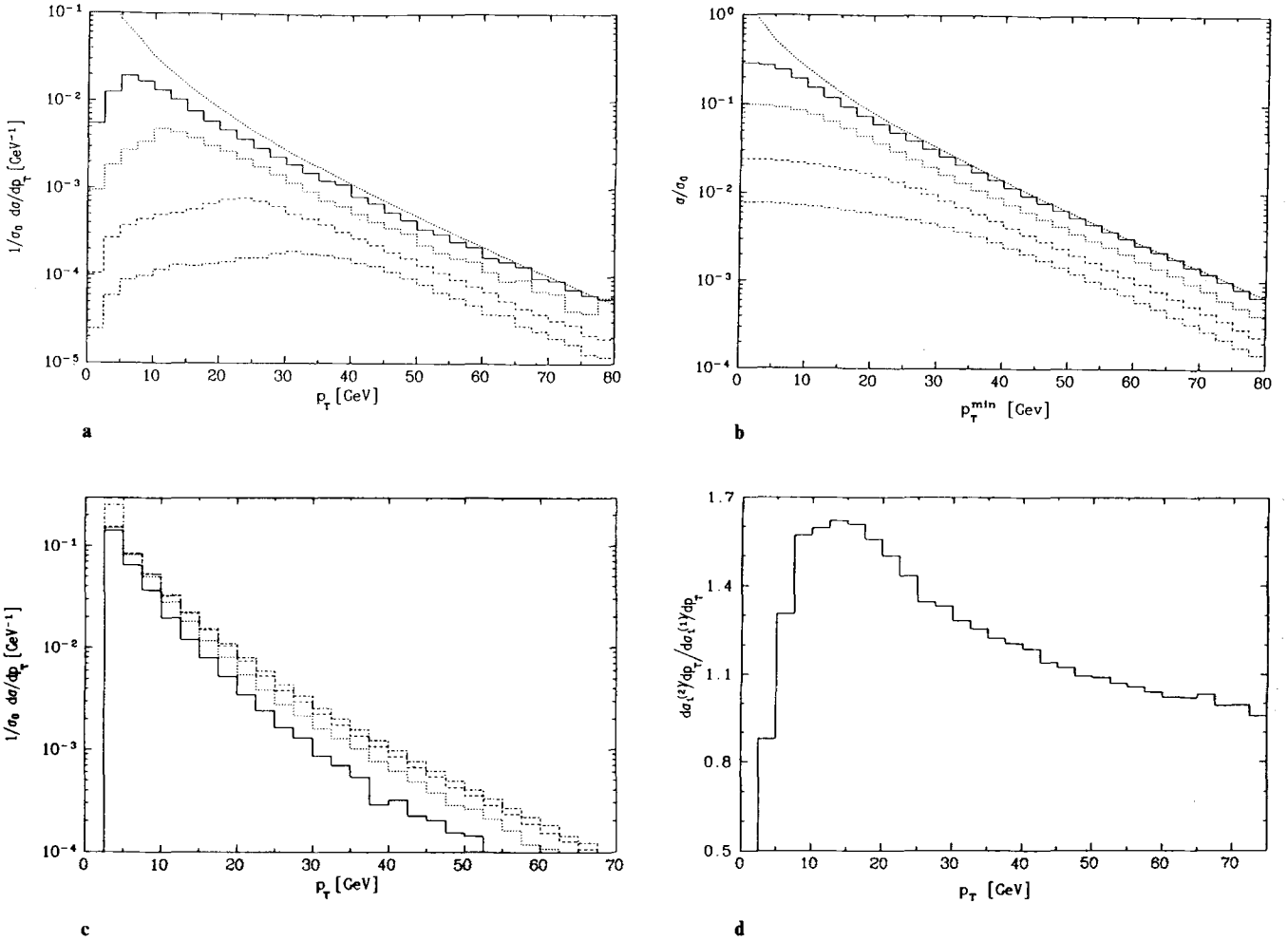

Fig. 2. **a** Same as Fig. 1a for Z-production ($\sigma_0 = 1.485$ nb). **b** Same as Fig. 1b for Z-production. **c** Same as Fig. 1c for Z-production. **d** Same as Fig. 1d for Z-production

the $O(\alpha_s)$ and the $O(\alpha_s^2)$ contribution which are evaluated with formulae of [8]. The results in Fig. 1a and Fig. 2a are qualitatively similar. The cross sections for W production are always somewhat larger than the cross sections for Z production. The cross sections exhibited in Fig. 1a and 2a have been integrated over the $p_T \equiv Q_T$ of the W and Z down to the value $p_T^{\min}$. The results of this integration are shown in Fig. 1b and 2b respectively. We see that for the smallest $p^j{}_{T\min} = 2.5$ GeV the integrated inclusive W and Z cross sections are almost totally given by the two-jet contribution if $p_T^{\min} > 60$ GeV. The higher order corrected 1-jet cross sections, as a function of p_T of the vector boson, which result from the subtraction of the 2-jet cross sections in Fig. 1a and Fig. 2a from the inclusive $(1+2)$-jet cross section, also given in Fig. 1a and 2a, are plotted in Fig. 1c and Fig. 2c. We see that for the smallest $p^j{}_{T\min} = 2.5$ GeV the 1-jet cross section as a function of p_T is much steeper than the $(1+2)$-jet cross section. For $p_T > 52$ Gev the $d\sigma_1/dp_T$ for Z-production becomes very small (see Fig. 2c). Having the 1-jet cross section $d\sigma_1/dp_T$ available it is of interest to compare this higher order cross section with the lower order cross section $d\sigma_1{}^{(1)}/dp_T$. This comparison is shown in Fig. 1d and 2d for W and Z production respectively. In these figures the differential cross section up to $O(\alpha_s^2)$ is denoted $d\sigma_1{}^{(2)}/dp_T$. We see that the ratio $(d\sigma_1{}^{(2)}/dp_T)/(d\sigma_1{}^{(1)}/dp_T)$ deviates from 1. This ratio varies as a function of p_T from 1.6 at $p_T = 25$ GeV to 1.0 at the highest $p_T = 75$ GeV, which we considered. So the higher order corrections are quite large and vary substantially as a function of p_T making the up to $O(\alpha_s^2)$ corrected distribution steeper than the lowest order distribution. The cut on $p^j{}_T$ was chosen equal to 10 GeV.

We have repeated the calculations for the Tevatron energy $\sqrt{S} = 1.8$ TeV. The equivalent curves are shown in Fig. 3a, b, c, d for W production and Fig. 4a, b, c, d for Z production. In Fig. 3a, b, c and 4a, b, c the cuts are $p^j{}_T \geqq 5, 10, 15, 20$ GeV, $\Delta R \geqq 0.7$ and $|\eta| \leqq 2.5$. The ratios $(d\sigma_1{}^{(2)}/dp_T)/(d\sigma_1{}^{(1)}/dp_T)$ are plotted in Fig. 3d (W production) and Fig. 4d (Z production) for $p^j{}_T \geqq 15$ GeV. The curves look similar as compared to the curves for $\sqrt{S} = 0.63$ TeV. The calculations were done up to $p_T = 150$ GeV instead of $p_T = 80$ GeV for the $Sp\bar{p}S$ collider.

For the lowest jet transverse momentum cut-off of

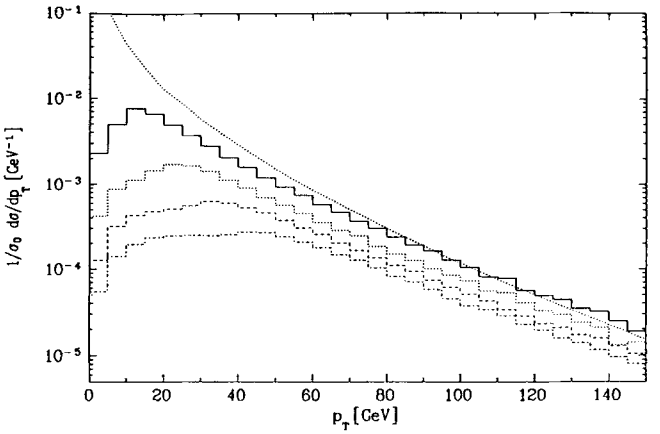

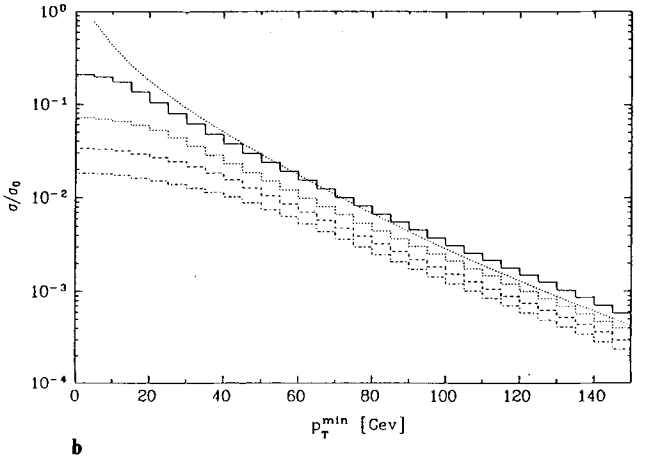

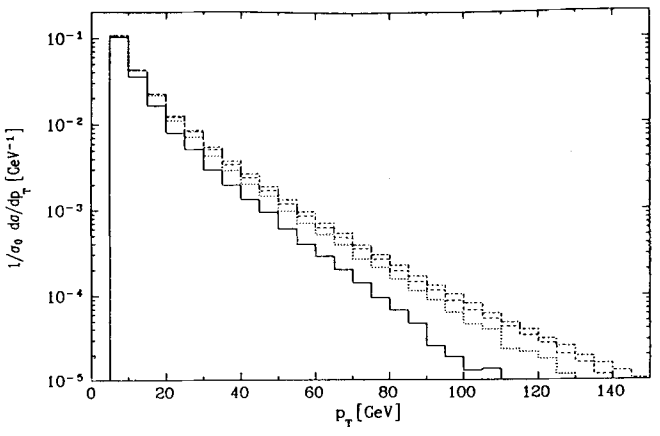

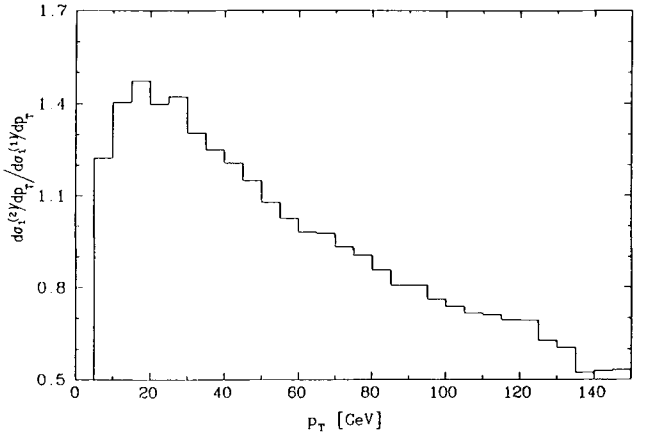

Fig. 3. **a** Same as Fig. 1a, now for $\sqrt{S} = 1.8$ TeV and $p^j{}_T \geqq 5, 10, 15, 20$ GeV, $\Delta R \geqq 0.7$ and $|\eta| \leqq 2.5$ ($\sigma_0 = 14.808$ nb). **b** Same as Fig. 1b, now for $\sqrt{S} = 1.8$ TeV and $p^j{}_T \geqq 5, 10, 15, 20$ GeV, $\Delta R \geqq 0.7$ and $|\eta| \leqq 2.5$. **c** Same as Fig. 1c, now for $\sqrt{S} = 1.8$ TeV and $p^j{}_T \geqq 5, 10, 15, 20$ GeV, $\Delta R \geqq 0.7$ and $|\eta| \leqq 2.5$. **d** Same as Fig. 1d, now for $\sqrt{S} = 1.8$ TeV, $p^j{}_T \geqq 15$ GeV, $\Delta R \geqq 0.7$ and $|\eta| \leqq 2.5$

5 GeV the p_T distribution for 2-jet production exceeds the p_T distribution for the inclusive (1 + 2)-jet production at $p_T = 100$ GeV. This is clearly seen in Fig. 3a and Fig. 4a and also in Fig. 3b and Fig. 4b where we plotted the integrated rates as a function of $p_T{}^{\min}$. This then leads to a negative 1-jet cross section for $p_T \gtrsim 100$ GeV in Fig. 3c and Fig. 4c. This result suggests that in this kinematic regime fixed-order perturbation theory breaks down for this small value of cut-off on $p^j{}_T$. In this region the $\alpha_s{}^2$ corrections for the 1-jet cross section are so large that we must assume that this cross section and the $O(\alpha_s{}^2)$ 2-jet cross section are substantically modified by $O(\alpha_s{}^3)$ corrections. Thus, while perturbation theory up to $O(\alpha_s{}^2)$ may be correct to describe the p_T distribution of the inclusive (1 + 2)-jet production, when no questions concerning the number of jets are asked, higher order corrections are needed to obtain reliable predictions for exclusive jet rates [3]. Similar inadequacies of $O(\alpha_s{}^2)$ perturbation theory for jet rates are also known in e^+e^- annihilation.

From the results presented in Fig. 1b, 2b, 3b and 4b we can read off the jet rates for 1 and 2 jets as a function of $p_T{}^{\min}$, the cut on the vector boson transverse momentum, for various cut-off values on $p^j{}_T$. These results can be compared with recently presented measurements of jet rates in W and Z production [1]. They have measured the fraction of events with a given number of jets:

$$f_n(V) = \frac{\sigma(V + n\,\text{jets})}{\sum_m \sigma(V + m\,\text{jets})}. \tag{4}$$

With a cut on the transverse energy of the jets of $E_T \geqq 7$ GeV the UA1 collaboration obtained from their sample of 357 W events the following jet rates: $f_0 = 0.63 \pm 0.05$, $f_1 = 0.29 \pm 0.05$, $f_2 = 0.065 \pm 0.015$ and $f_3 = 0.017 \pm 0.008$, so that 37% of the W events have at least one jet with $E_T \geqq 7$ GeV. From these numbers we get: $f_1/f_0 = 0.46 \pm 0.12$ and $f_2/f_0 = 0.10 \pm 0.02$. We compare these numbers with the jet rates σ_1/σ_0 and σ_2/σ_0 for $p^j{}_T \geqq 5$ GeV and $p_T{}^{\min} \geqq 5$ GeV. With these cuts we model the actual jet $E_T{}^{\min}$ of 7 GeV used in the UA1 measurements [4]. The cuts on ΔR and $|\eta|$ are the same as in the actual measurements. From Fig. 1b (and also Table 1) we get: $\sigma_1/\sigma_0 = 0.43$ and $\sigma_2/\sigma_0 = 0.086$ in resonable agreement with the experimental data. This should, however, not be considered a precise comparison. First we are calculating at the parton level taking no account

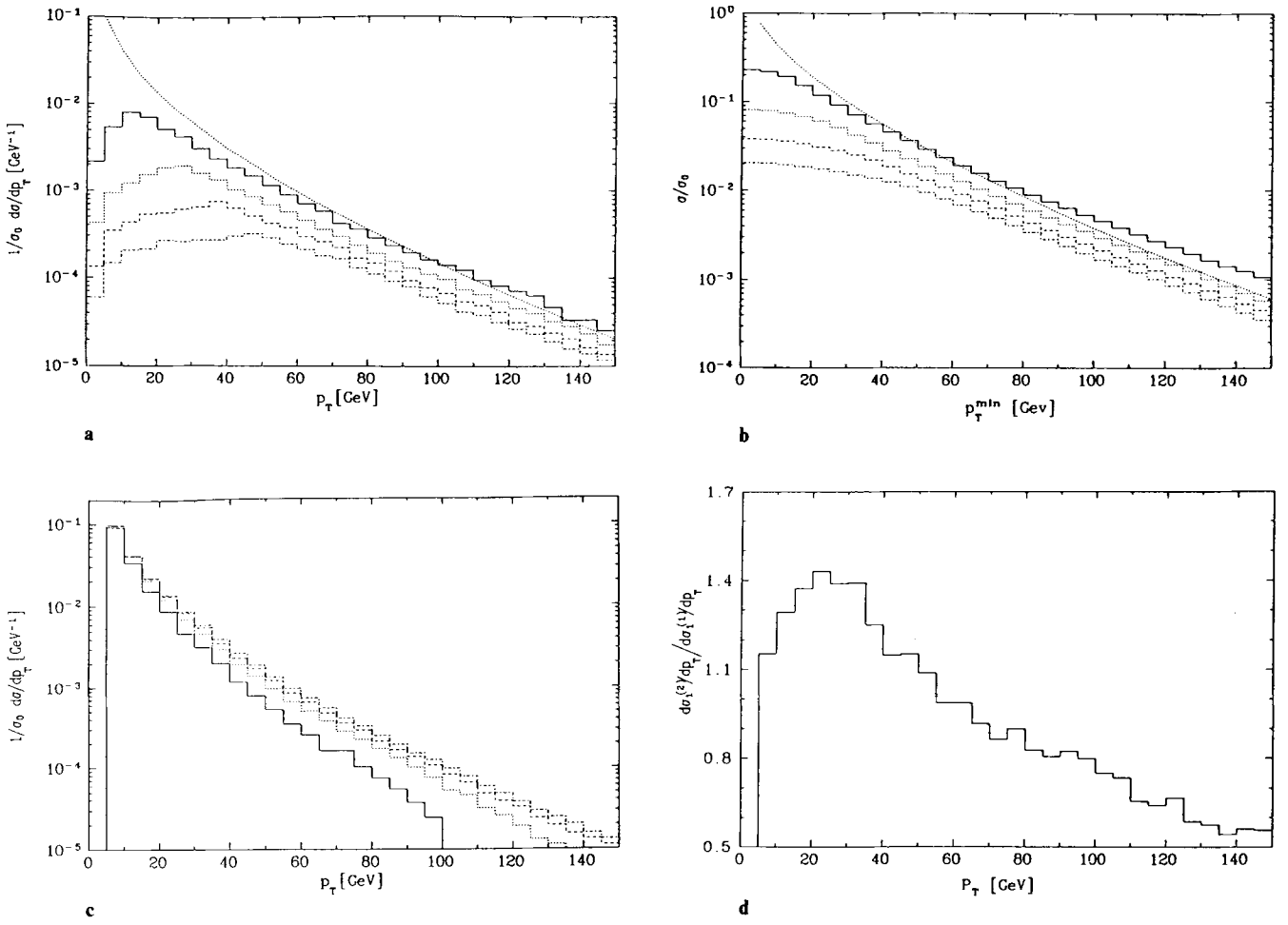

Fig. 4. **a** Same as Fig. 3a for Z-production ($\sigma_0 = 4.647$ nb). **b** Same as Fig. 3b for Z-production. **c** Same as Fig. 3c for Z-production. **d** Same as Fig. 3d for Z-production

of fragmentation, smearing, resolution and exact experimental cuts. Second we describe the cross section σ_0 with no extra jet by the lowest order contribution. This cross section is also changed by higher order corrections of $O(\alpha_s)$ and $O(\alpha_s^2)$. They determine the K-factor K_0. This K-factor has been calculated up to $O(\alpha_s)$ [2]. It turns out that for $p_T{}^{\min} = 5\,\text{GeV}$ $K_0 \simeq 1.0$. The UA1 collaboration measured also f_0, f_1 and f_2 for Z production + jets [1]. From these data we deduce $f_1/f_0 = 0.59 \pm 0.22$ and $f_2/f_0 = 0.16 \pm 0.10$. This must be compared with $\sigma_1/\sigma_0 = 0.43$ and $\sigma_2/\sigma_0 = 0.096$ taken from Fig. 2b (and also from Table 1) which are in agreement with the data.

In order to get an idea how these jet fractions depend on the structure function input we have repeated the calculations with the MRS EB mode 1 structure functions which correspond to the fit to the EMC data with $\Lambda_{\overline{\text{MS}}} = 0.1\,\text{GeV}$ [12]. The results are also shown in Table 1. σ_1/σ_0 is decreased somewhat, approximately by 7%. The change of σ_2/σ_2 is larger, up to 15% at $\sqrt{S} = 0.63\,\text{TeV}$.

We can also compare our values of f_1/f_0 (for W-production) which contains the $O(\alpha_s^2)$ corrections with the tree-graph results of Berends et al. [4]. They obtained with the same cuts and the very similar structure functions (MRS B, $\Lambda_{\overline{\text{MS}}} = 0.2\,\text{GeV}$) $f_1/f_0 = 0.34$ which must be compared to our $\sigma_1/\sigma_0 = 0.43$. So the higher order corrections lead to an increase of σ_1 by 25% for the particular cuts chosen. Unfortunately the experimental accuracy is still not sufficient to detect the effect of the $O(\alpha_s^2)$ contribution in σ_1. We note that our value for σ_1 is in better agreement with the data than the tree-graph result.

Table 1. Comparison of jet fractions $\sigma_1{}^V/\sigma_0{}^V$ and $\sigma_2{}^V/\sigma_0{}^V$ for $V = W, Z$ production at $\sqrt{S} = 0.63\,\text{TeV}$ and $\sqrt{S} = 1.8\,\text{TeV}$ for two structure function sets, mode 1 and mode 2 of MRS EB [12]. The cuts on $p^j{}_T$ are 5 GeV (10 GeV) for $\sqrt{S} = 0.63\,\text{TeV}$ (1.8 TeV)

$\sqrt{S}$	0.63 TeV		1.8 TeV	
Mode	1	2	1	2
σ_1^W/σ_0^W	0.396	0.430	0.337	0.357
σ_1^Z/σ_0^Z	0.406	0.431	0.338	0.349
σ_2^W/σ_0^W	0.075	0.086	0.064	0.069
σ_2^Z/σ_0^Z	0.088	0.096	0.072	0.078

Other experimental data on $W+n$ jet production have been obtained by the UA2 collaboration. They have recently reported a measurement of the strong coupling α_s from the relative rate of $W+1$ jet production [2]. This analysis is very involved and cannot be repeated here. Their measurement of α_s also relies on the knowledge of K-factors for 1- and 0-jet production. Their calculation of the factor K_1 taking into account the $O(\alpha_s^2)$ corrections for $W+1$ jet production was based only on the non-singlet contributions of Ellis et al. [6]. In this connection it is of interest to know the change of K_1 if all singlet and non-singlet contributions are included. To see how large this change is we have calculated

$$K(p_T{}^W)=\frac{d\sigma^{(2)}}{dp_T{}^W}\Big/\frac{d\sigma^{(1)}}{dp_T{}^W} \tag{5}$$

where $d\sigma^{(2)}/dp_T{}^W$ is the complete $(1+2)$-jet transverse momentum distribution, shown in Fig. 1a, and $d\sigma^{(1)}/dp_T{}^W$ is this distribution in $O(\alpha_s)$ only. This function is compared with the equivalent function taking only non-singlet contributions in the numerator and in the denominator into account. The result of this comparison is shown in Fig. 5. We see that for $\sqrt{S}=0.63$ TeV the $K(p_T{}^W)$ including all contributions differs only very little. At the highest $p_T{}^W=100$ GeV the difference from the approximate $K(p_T{}^W)$ based on the non-singlet terms is larger, of the order of 7%. Since the main contribution to the correction factor K_1 comes from the smaller $p_T{}^W$ the net effect is even smaller. We observe that at higher energies the difference between the complete $K(p_T{}^W)$ and the approximate non-singlet $K(p_T{}^W)$ increases. At $\sqrt{S}=16$ TeV it is of the order of 20% for $p_T{}^W=100$ GeV. Concerning the evaluation of α_s from the $W+1$ jet rate in [2] we can conclude that their result will change very little by including the singlet terms in their calculation of K_1 and their error estimate $\Delta K_1=0.2$ originating from the approximation of the K_1 factor calculations is too large.

We calculated the K_1 factor as a function of $p_T{}^{\min}$ for the MRS EB mode 2 structure functions [12] for the case $\omega_{12}>20°$. The result is exhibited in Fig. 6. We find agreement with the result of the UA2 collaboration [2] up to a small deviation not exceeding 5%. This difference is presumably due to the extra contribution of the singlet terms and the use of different structure functions as compared to [2]. In Fig. 6 we also show the limiting curve which comes out when the minimum $p^j{}_T$ is very large, i.e. when there is no 2-jet contribution subtracted. We conclude that the contribution of the singlet contribution, which were left out in the evaluations of [2], are not very important. Therefore the results of [2] are quite reliable and the error estimate $\Delta K_1=0.2$ assumed in [2] for their calculation of K_1 is certainly too large. That K_1 changes so little when the singlet contributions are included does not mean that these terms are irrelevant. They just cancel in the ratio (5). In $O(\alpha_s)$ they are important even for $\sqrt{S}=0.63$ TeV and must be taken into account.

Finally we emphasize that our definition of the 1-jet and 2-jet cross section always has the requirement that the transverse momentum of the vector boson $p_T{}^V$ is larger than some $p_T{}^{\min}$. All contributions with $p_T<p_T{}^{\min}$ are considered as part of the cross section with no jet.

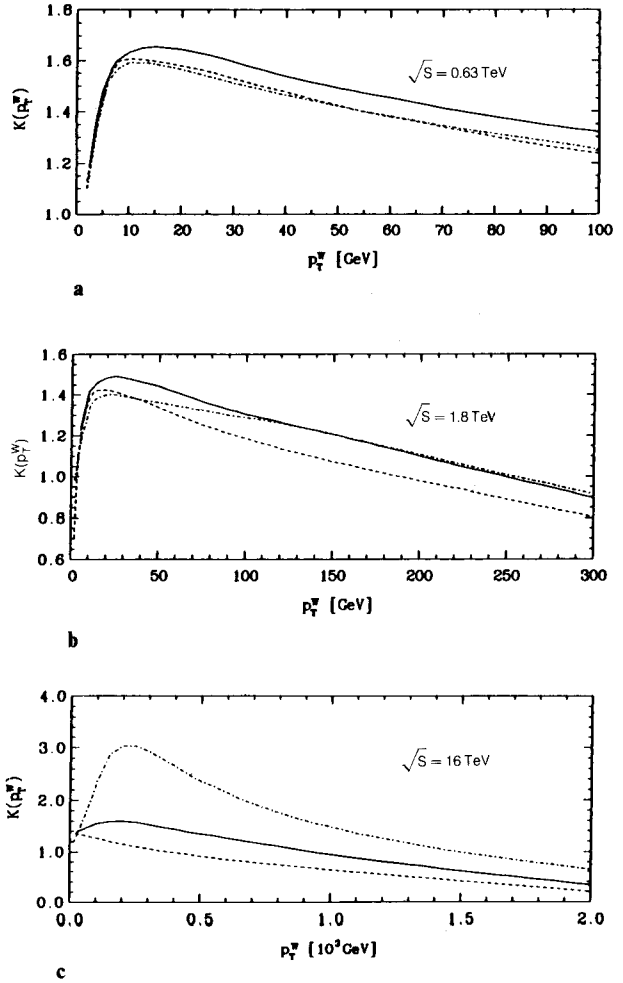

Fig. 5a–c. $K(p_T{}^W)$ as defined in (5) as a function of $p_T{}^W$ for sum of singlet and non-singlet contribution (full curve), non-singlet contribution (dashed curve) and only valence quarks (dashed-dotted curve) for **a** $\sqrt{S}=0.63$ TeV, **b** $\sqrt{S}=1.8$ TeV and **c** $\sqrt{S}=16$ TeV

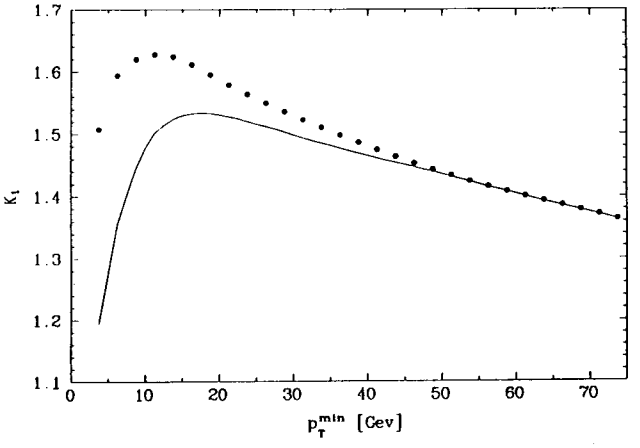

Fig. 6. The K_1 factor of [2] as a function of $p_T{}^{\min}$ for the MRS EB mode 2 [12] structure function with all singlet contributions included. The full points giving the limiting curve for K_1 are obtained for cut-off on $p^j{}_T$ becoming large

This selection criterion is fully correct for the $O(\alpha_s)$ cross section. In $O(\alpha_s^2)$, however, there are event configurations where two partons are emitted and obey $p^1{}_T > p_T{}^{\min}$, $p^2{}_T < p_T{}^{\min}$, $\omega_{12} > \omega^{\min}$, $p_T{}^V < p_T{}^{\min}$. Topologically one would count this as part of the 1-jet configuration. A similar ambiguity holds for the configuration $p^1{}_T < p_T{}^{\min}$, $p^2{}_T < p_T{}^{\min}$, $\omega_{12} > \omega^{\min}$, $p_T{}^V > p_T{}^{\min}$ which we include in our 1-jet sample which should be considered as part of the zero-jet cross section. It is, however, a matter of definition how we define the 1-jet configuration.

Acknowledgements. F.T. Brandt and S.-L. Nyeo would like to thank the Alexander von Humboldt Foundation for the financial support. We are grateful to R.J. Gonsalves and W.J. Stirling for sending us computer codes of their work.

References

1. C. Albajar et al. UA1 Coll.: Z. Phys. C – Particles and Fields 44 (1989) 15
2. R. Ansari et al. UA2 Coll.: Phys. Lett. B215 (1988) 175, K. Jakobs, Dissertation, University of Heidelberg, 1988 (unpublished)
3. S.D. Ellis, R. Kleiss, W.J. Stirling: Phys. Lett. B154 (1985) 435; Phys. Lett. B163 (1985) 261; R. Kleiss, W.J. Stirling: Nucl. Phys. B262 (1985) 235; Phys. Lett. B180 (1986) 171
4. V. Barger, T. Han, J. Ohnemus, D. Zeppenfeld: Phys. Rev. Lett. 62 (1989) 1971; F.A. Behrends et al.: Phys. Lett. B224 (1989) 237
5. T. Matsuura, S.C. van Marck, W.L. van Neerven: Phys. Lett. B211 (1988) 171; Nucl. Phys. B319 (1989) 570
6. R.K. Ellis, G. Martinelli, R. Petronzio: Nucl. Phys. B211 (1983) 106
7. P.B. Arnold, M.H. Reno: Nucl. Phys. B319 (1989) 37. See also P.B. Arnold, R.K. Ellis, M.H. Reno: Phys. Rev. D40 (1989) 912
8. R.J. Gonsalves, J. Pawlowski, C.-F. Wai: Phys. Rev. D40 (1989) 2245
9. R.K. Ellis et al.: Nucl. Phys. B152 (1979) 285; D. Amati, R. Petronzio, G. Veneziano: Nucl. Phys. B146 (1978) 29
10. G. Altarelli, R.K. Ellis, G. Martinelli: Nucl. Phys. B157 (1979) 461; B. Humpert, W.L. van Neerven: Nucl. Phys. B184 (1981) 225
11. G. Kramer, B. Lampe: Z. Phys. C – Particles and Fields 34 (1987) 497
12. A.D. Martin, R.G. Roberts, W.J. Stirling: Mod. Phys. Lett. A4 (1989) 1135. For earlier versions see Phys. Rev. D37 (1988) 1161; Phys. Lett. B206 (1988) 327
13. Review of Particle Properties: Phys. Lett. B204 (1988) 96